

Passivation of GaAs using $(\text{Ga}_2\text{O}_3)_{1-x}(\text{Gd}_2\text{O}_3)_x$, $0 \leq x \leq 1.0$ films

J. Kwo, D. W. Murphy, M. Hong, R. L. Opila, J. P. Mannaerts, A. M. Sergent,
and R. L. Masaitis

Bell Laboratories, Lucent Technologies, Murray Hill, New Jersey 07974

(Received 19 April 1999; accepted for publication 30 June 1999)

The $\text{Ga}_2\text{O}_3(\text{Gd}_2\text{O}_3)_x$ dielectric film was previously discovered to passivate the GaAs surface effectively. We have investigated the systematic dependence of the dielectric properties of $(\text{Ga}_2\text{O}_3)_{1-x}(\text{Gd}_2\text{O}_3)_x$ on the Gd (x) content. Our results show that pure Ga_2O_3 does not passivate GaAs. Films with $x \geq 14\%$ are electrically insulating with low leakage current and high electrical breakdown strength. Furthermore, a low interfacial density of states was attained in films with $x \geq 14\%$. The results show the important role of Gd_2O_3 in the $(\text{Ga}_2\text{O}_3)_{1-x}(\text{Gd}_2\text{O}_3)_x$ dielectric films for effective passivation of GaAs. © 1999 American Institute of Physics.
[S0003-6951(99)04434-4]

Effective passivation of III–V compound semiconductors finds applications in photonic and electronic devices. Intensive efforts have been made over the last 35 years in searching for electrically and thermodynamically stable insulators on GaAs and other related III–V compound semiconductors.^{1–5} A heterostructure of an insulator/III–V compound semiconductor with a low interfacial state density D_{it} would provide a basis for the long-sought metal–oxide–semiconductor field-effect transistors (MOSFETs) in III–V compound semiconductors. However, direct oxidation of GaAs surface by means of the thermal, anodic, and plasma methods inevitably form oxides containing arsenic oxides, leading to strong Fermi surface pinning. Furthermore, deposition of the stable, better known oxide films such as MgO , SiO_2 , and Al_2O_3 on the GaAs surface does not form a heterostructure with a low D_{it} .^{6,7} Remarkably, *in situ* deposition of $\text{Ga}_2\text{O}_3(\text{Gd}_2\text{O}_3)_x$ dielectric film on GaAs surfaces produced MOS diode structures^{6,8} with a low D_{it} . Subsequent employment of the $\text{Ga}_2\text{O}_3(\text{Gd}_2\text{O}_3)_x$ as a gate dielectric along with an ion implantation process led to the demonstration of the enhancement-mode GaAs MOSFETs with inversion on semi-insulating GaAs substrates in both *n*- and *p*-channel configurations.⁹

The fundamental reason for such a remarkably low D_{it} at the $\text{Ga}_2\text{O}_3(\text{Gd}_2\text{O}_3)_x/\text{GaAs}$ interface is not clear. Stable, insulating dielectric layers on GaAs, as formed by electron beam evaporation of $\text{Gd}_3\text{Ga}_5\text{O}_{12}$ (GGG) garnet were initially thought to result from the preferential evaporation of Ga_2O_3 since the vapor pressure of Ga_2O_3 is much higher than that of Gd_2O_3 . This was thought to give rise to formation of higher purity Ga_2O_3 film than possible from evaporation of a powder-packed Ga_2O_3 source. However, chemical analysis of our effective passive films indicated the presence of a considerable amount of Gd (as high as 20–40 at %). This raised the question of the importance of Gd_2O_3 to GaAs surface passivation.

In this work we have studied of the dependence of the dielectric properties of $(\text{Ga}_2\text{O}_3)_{1-x}(\text{Gd}_2\text{O}_3)_x$ films on the Gd (x) content. The current–voltage (*I*–*V*) and capacitance–voltage (*C*–*V*) results show that pure Ga_2O_3 films have poor electrical leakage properties, and do not passivate the GaAs

surface. Additions of Gd with $x \geq 14\%$ improved the dielectric performance greatly in terms of the leakage current density and the electrical breakdown field strength. Our results suggest that Gd_2O_3 is a necessary component that helps to stabilize the $(\text{Ga}_2\text{O}_3)_{1-x}(\text{Gd}_2\text{O}_3)_x$ film chemically due to the electropositive nature of Gd^{+3} , thus giving electrically insulating behavior.

The growth of mixed oxides $(\text{Ga}_2\text{O}_3)_{1-x}(\text{Gd}_2\text{O}_3)_x$ with $x = 0–1.0$ on GaAs was performed in a multichamber UHV system described previously.^{6,10} Reflection high-energy electron diffraction (RHEED) was used to monitor film growth of both GaAs epilayer and oxide films. Prior to oxide deposition either an As-stabilized (2×4) or a Ga-stabilized (4×6) reconstructed surface was obtained after heating to 550 °C or above. Substrate temperature was held at 450–550 °C during the oxide growth. Both approaches of e-beam evaporation from a single source and coevaporation from two sources were employed. Various oxide charges were used including a single crystal GGG, a powder packed composite oxide consisting of $(\text{Ga}_2\text{O}_3)_{1-x}(\text{Gd}_2\text{O}_3)_x$ with a composition close to $\text{Ga}_5\text{Gd}_3\text{O}_{12}$, and powder packed pure Gd_2O_3 and pure Ga_2O_3 sources.

Oxide film thickness was measured by ellipsometry and x-ray reflectivity.¹¹ The film composition was determined by using Rutherford backscattering spectrometry (RBS) and Auger electron spectroscopy. The MOS diode structure was fabricated by evaporating Au/Pt dots 75, 100, 150 μm in diameter to the oxide film surface for electrical contacts. The *I*–*V* and *C*–*V* measurements were taken using the standard procedures described previously.^{10,11}

When evaporated from a single source of GGG, the Gd composition in the deposited films depended on the usage of the source and the substrate temperatures. Thus, precise control of the film composition was quite limited, as noted by the variation of Gd composition in Fig. 1. Since the melting point of Gd_2O_3 is much higher than that of Ga_2O_3 , after repeated runs Gd-rich material was left in the charge. We also observed an increased content of Gd oxide in the films at higher substrate temperatures, due to a higher sticking coefficient of Gd_2O_3 . It is much easier to control the film compositions by coevaporation from two separate sources.

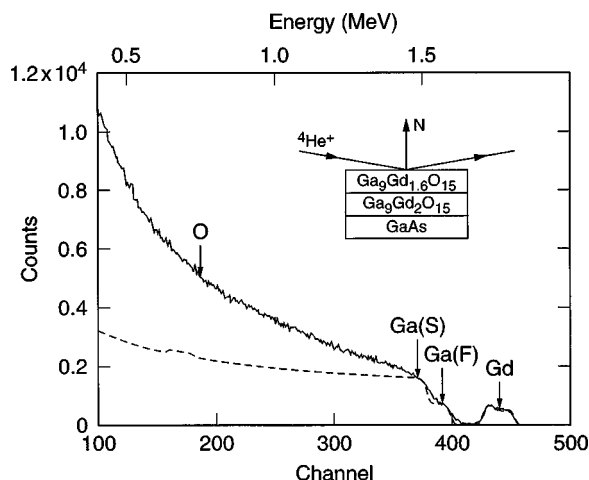


FIG. 1. RBS spectrum for a $(\text{Ga}_2\text{O}_3)_{83}(\text{Gd}_2\text{O}_3)_{17}$ film 160 Å thick with the incident $^4\text{He}^+$ ion beam directed at 83.5° to the film normal. The Ga edges for the film and the substrate are denoted as Ga(F) and Ga(S), respectively.

The evaporation rate from each source can be individually adjusted.

We note that both the oxide film and the substrate contain the Ga species. In order to resolve the Ga edge of thin oxide film from that of the substrate in the RBS spectrum, the substrate plane was rotated so that the $^4\text{He}^+$ ion beam was incident at an angle $\theta \sim 80^\circ - 85^\circ$ to the substrate normal. The effective film thickness is enhanced by a factor of $(1/\cos \theta)$. Figure 1 shows a RBS spectrum taken using a 2.0 MeV $^4\text{He}^+$ ion beam for a $\text{Ga}_2\text{O}_3(\text{Gd}_2\text{O}_3)$ sample 160 Å thick, e-beam evaporated from GGG. The incident angle of the ion beam is set at 83.5° to the substrate normal to separate the two Ga edges. A variation of Gd composition in the oxide is detected in the depth profile. The best fit to the spectrum by the RUMP program indicates a bilayer profile, consisting of an upper layer of approximately $\text{Ga}_9\text{Gd}_{1.6}\text{O}_{15}$ 80 Å thick, and a lower layer of approximately $\text{Ga}_9\text{Gd}_2\text{O}_{15}$ 80 Å thick near the GaAs interface. The average Gd composition x is $\sim 17\%$. Auger measurements on our passive films of $(\text{Ga}_2\text{O}_3)_{1-x}(\text{Gd}_2\text{O}_3)_x$ indicate the presence of a considerable quantity of Gd, and the Gd to Ga composition ratio is consistent with the RBS results.

Figure 2 shows J_L-E characteristics for a set of $(\text{Ga}_2\text{O}_3)_{1-x}(\text{Gd}_2\text{O}_3)_x$ films on GaAs with x systematically increased from 0%, 6%, 14%, 20%, to 100%. All the mixed-oxide films (6%, 14%, and 20%) are structurally amorphous from RHEED studies. The pure Gd_2O_3 sample is an epitaxial, single crystalline film, and the pure Ga_2O_3 is a polycrystalline film with a preferred orientation. The film thickness is kept close to 200 Å for all Gd-added samples. The positive bias means that the top metal electrode (Pt/Au) is positive with respect to GaAs. Pure Ga_2O_3 films show very high leakage current with poorly defined breakdown characteristics. Small additions of Gd with $x=6\%$ and 14% to the dielectric films drastically reduced the leakage current density by 3 or 4 orders of magnitude and also increased the breakdown field strength. The $x=20\%$ sample showed a low leakage current density in the range of $10^{-8} - 10^{-9} \text{ A/cm}^2$ prior to breakdown, and an electrical breakdown field E_{br} of 2.5 MV/cm. Interestingly, pure Gd_2O_3 film showed even lower leakage current density by 1 order of magnitude when compared to

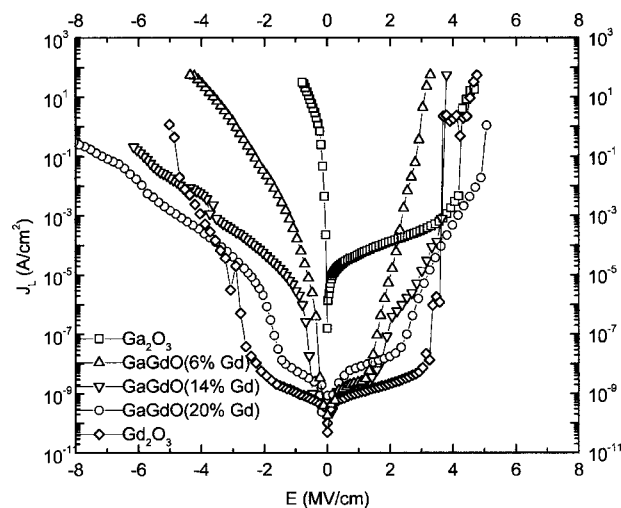


FIG. 2. Dependence of leakage current density J_L on the electric field E for a set of $(\text{Ga}_2\text{O}_3)_{1-x}(\text{Gd}_2\text{O}_3)_x$ films with x varying from 0%, 6%, 14%, 20%, to 100%.

the $x=20\%$ sample, and the breakdown behavior is characteristics of a hard breakdown with an E_{br} increased to 3.5 MV/cm. Based on our $J-E$ results, we conclude that Gd_2O_3 is necessary for electrically insulating films. A full account on the passivation of GaAs by the epitaxial Gd_2O_3 film was given in a separate article.¹²

Figures 3(a)–3(d) show the results of $C-V$ measurements for passive films of $x=6\%$, 14%, 20%, and 100%, respectively. The operations in accumulation, depletion, and inversion are evident for the $x=14\%$, 20%, and 100% samples at frequencies varying from 50 Hz to 1 MHz. The $C-V$ characteristics were analyzed by taking the conductance G into account. The finite value of G is in parallel with the oxide capacitance C_{ox} . This simple equivalent circuit model explains that the total capacitance increases as the modulation frequency decreases. After replotting the $C-V$ curves by subtracting the contributions from G and C_{ox} , the interfacial density of states D_{it} , which responds only to the low-frequency measurements, can be deduced from the high- and low-frequency curves. The D_{it} at the mid-gap is about $\sim 10^{11} \text{ cm}^{-2} \text{ eV}^{-1}$ for the $x=100\%$ sample. For the samples of $x=20\%$ and 14%, the D_{it} values are less than $10^{11} \text{ cm}^{-2} \text{ eV}^{-1}$. In contrast, pure Ga_2O_3 samples are too resistively leaky to give meaningful $C-V$ data. The $x=6\%$ sample did not show the $C-V$ curves expected for an unpinned oxide/GaAs interface.

Bulk Ga oxides are known to contain essentially only Ga^{3+} , and this is confirmed in our Ga_2O_3 films by XPS,¹³ where the sensitivity of XPS to other oxidation states of Ga is limited to $\sim 1\%$. However, the number of oxygen vacancies, and hence the electrical conductivity, may depend strongly on the preparation environment.^{13–15} During e-beam evaporation of $(\text{Ga}, \text{Gd})_2\text{O}_3$, the oxygen partial pressure in the growth system rose to a level of 10^{-9} Torr. This may lead to oxygen vacancies in the films and/or a small amount of reduced Ga. Traps due to oxygen vacancies may cause the high electrical leakage in films of pure gallium oxide. It is well known that additions of electropositive elements in ternary phases stabilize high oxidation states for metals with multiple oxidation states. Examples are given in BaPbO_3 ,

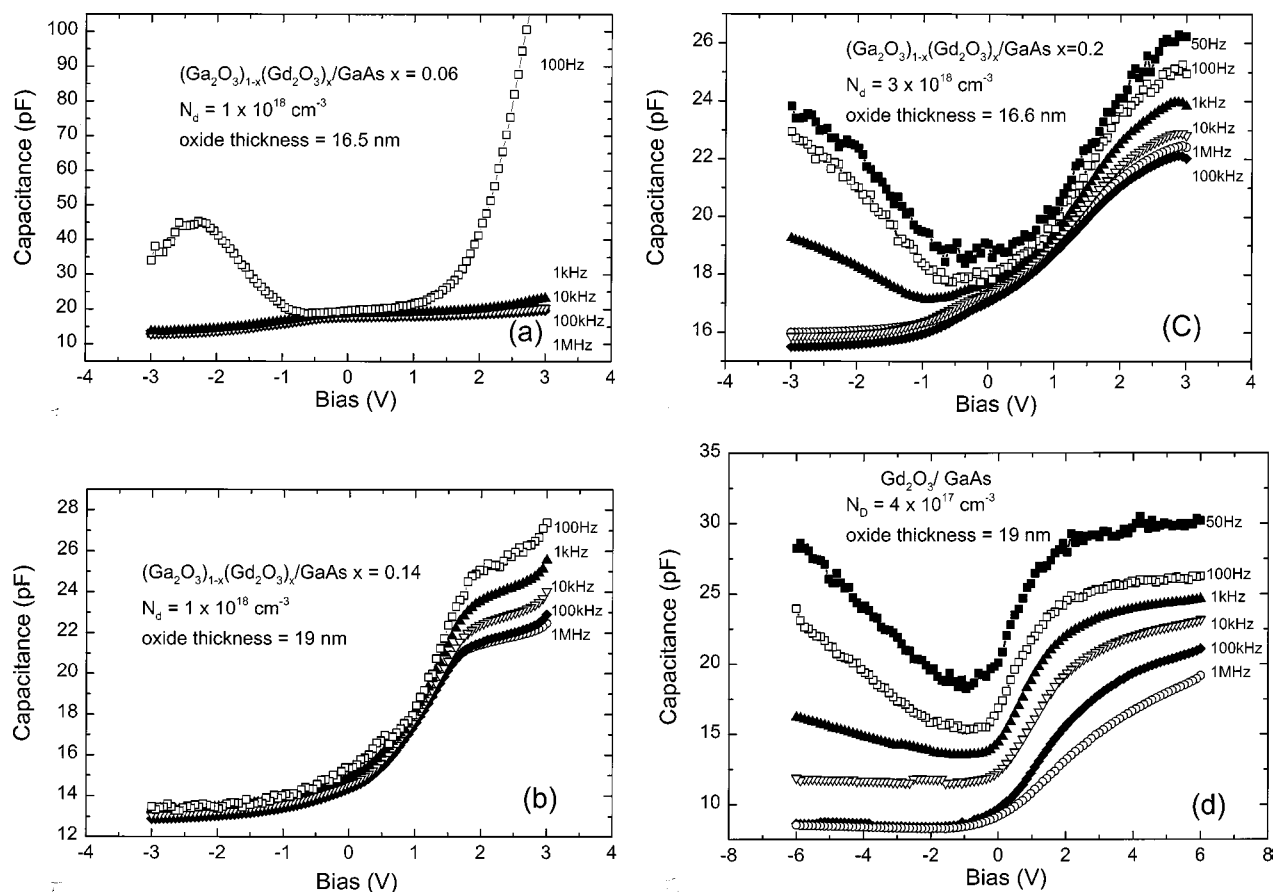


FIG. 3. C - V curves as a function of frequency from 50 Hz to 1 MHz for a set of $(\text{Ga}_2\text{O}_3)_{1-x}(\text{Gd}_2\text{O}_3)_x$ films with (a) $x=6\%$, (b) 14%, (c) 20%, and (d) 100%. The area of the capacitor is $4.4 \times 10^{-5} \text{ cm}^2$.

$\text{YBa}_2\text{Cu}_3\text{O}_7$, KMnO_4 , and SrFeO_3 . On this basis we suggest that Gd (Pauling electronegativity 1.1) minimizes oxygen vacancies, or is equivalent to maximizing the Ga oxidation state. An earlier work also found that inclusion of MgO and ZrO_2 (electronegativities 1.2 and 1.4, respectively, for Mg and Zr) reduces the conductivity of bulk single-crystal Ga_2O_3 .¹⁴ This proposition satisfactorily explains our electrical results and suggests, contrary to previous thinking that Gd was a problematic dopant,¹⁶ that Gd is beneficial. Furthermore, films containing other codeposited electropositive metal oxides may also give passive films. Of the possible electropositive elements, rare earth and alkaline earth elements are preferred over alkali metals because of stability to moisture and compatibility with other processing considerations.

In conclusion, we show in this work that the oxide which effectively passivates GaAs is not pure gallium oxide, but instead, contains a considerable amount of Gd_2O_3 exceeding 14%. Our results suggest that Gd_2O_3 is necessary in either reducing the oxygen vacancies or stabilizing gallium oxide to be in the 3^+ state. Based on our findings, we propose the passivating oxide to have the general composition of $\text{Ga}_{1-x}\text{A}_x\text{O}_2$, where A is an electropositive stabilizing element adapted for stabilizing Ga in the 3^+ oxidation state, and could preferably be the rare earth and alkaline earth elements.

The authors would like to thank R. M. Fleming for RBS and A. R. Kortan for x-ray diffraction analysis.

- ¹A. Revesz and K. Zaininger, *J. Am. Ceram. Soc.* **46**, 606 (1963).
- ²O. Weinreich, *J. Appl. Phys.* **37**, 2924 (1966).
- ³T. Mimura, K. Odani, N. Yokoyama, Y. Nakayama, and M. Fukuta, *IEEE Trans. Electron Devices* **25**, 573 (1978).
- ⁴W. T. Tsang, *Appl. Phys. Lett.* **33**, 429 (1978).
- ⁵*Physics and Chemistry of III-V Compound Semiconductor Interfaces*, edited by C. W. Wilmsen (Plenum, New York, 1985).
- ⁶M. Hong, M. Passlack, J. P. Mannaerts, J. Kwo, S. N. G. Chu, N. Moriya, S. Y. Hou, and V. J. Fratello, *J. Vac. Sci. Technol. B* **14**, 2297 (1996).
- ⁷L. W. Tu, E. F. Schubert, M. Hong, and G. J. Zyzdik, *J. Appl. Phys.* **80**, 6448 (1996).
- ⁸M. Passlack, M. Hong, J. P. Mannaerts, J. Kwo, R. L. Opila, S. N. G. Chu, N. Moriya, and F. Ren, *IEEE Trans. Electron Devices* **44**, 214 (1997).
- ⁹F. Ren, M. Hong, W. S. Hobson, J. M. Kuo, J. R. Lothian, J. P. Mannaerts, J. Kwo, Y. K. Chen, and A. Y. Cho, *Tech. Dig. Int. Electron Devices Meet.*, 943 (1996).
- ¹⁰M. Hong, *J. Cryst. Growth* **150**, 277 (1995).
- ¹¹M. Hong, M. A. Marcus, J. Kwo, J. P. Mannaerts, A. M. Sergent, L. J. Chou, K. C. Hsieh, and K. Y. Cheng, *J. Vac. Sci. Technol. B* **16**, 1395 (1998).
- ¹²M. Hong, J. Kwo, A. R. Kortan, J. P. Mannaerts, and A. M. Sergent, *Science* **283**, 1897 (1999).
- ¹³M. Fleischer and H. Meixner, *J. Appl. Phys.* **74**, 300 (1993).
- ¹⁴T. Harwig and J. Schoonman, *J. Solid State Chem.* **23**, 205 (1978).
- ¹⁵L. N. Cojocaru and I. D. Alecu, *Z. Phys. Chem. (Munich)* **84**, 325 (1973).
- ¹⁶M. Passlack and J. K. Abrokwhah, U.S. patent No. 5,597,768 (28 January 1997).